

## Detection of Melanoma Cells Displaying Multiple Genomic Changes in Histopathologically Negative Sentinel Lymph Nodes

Anja Ulmer,<sup>1</sup> Jörg R. Fischer,<sup>2</sup> Stefan Schanz,<sup>1</sup> Karl Sotlar,<sup>3</sup> Helmut Breuninger,<sup>1</sup> Klaus Dietz,<sup>4</sup> Gerhard Fierlbeck,<sup>1</sup> and Christoph A. Klein<sup>2</sup>

**Abstract Purpose:** Improved detection of early-disseminated melanoma cells may eventually translate into more effective patient care. We present a novel strategy for detection of melanoma cells in sentinel lymph nodes and confirm their malignant descent by genomic characterization.

**Experimental Design:** In sentinel lymph nodes from 358 melanoma patients, we prospectively compared the rates of tumor cell detection between immunocytochemistry using HMB45 and Melan A antibodies on disaggregated lymph node samples and standard histopathology (H&E staining and immunostaining on tissue sections). Immunocytochemical melanoma cell detection was controlled by testing lymph node samples from 59 nonmelanoma patients and by isolation and comparative genomic analysis of 30 antigen-positive cells.

**Results:** Of the 358 patients, 43 (12%) were positive by standard histopathology, whereas HMB45 immunocytochemistry detected 159 of 358 (44%) positive patients. None of the control samples reacted with the HMB45 antibody. Reexamination of samples that were classified as negative by histopathology revealed that extensive serial sectioning would be necessary to achieve sensitivity similar to HMB45 immunocytochemistry. Interestingly, both the number of immunocytochemically positive samples and the number of positive cells in the sentinel node correlated with the thickness of the primary tumor ( $r = 0.34$ ;  $P = 0.001$  and  $P < 0.0001$ , respectively). Twenty-four of 30 isolated immunocytochemically positive cells (80%) displayed chromosomal aberrations, some of which were isolated from histopathologically negative nodes.

**Conclusion:** Immunocytochemical detection of melanoma cells in sentinel lymph nodes is superior to standard histopathology. It remains to be determined whether the detection and genomic characterization of isolated melanoma cells in sentinel lymph nodes will provide relevant prognostic information.

Sentinel lymph node biopsy is a surgical technique for detecting micrometastatic disease in draining regional lymph nodes. It has been widely accepted as the preferred method to determine the pathologic status of the regional lymph nodes in patients with malignant melanoma and the resulting information has been incorporated into the latest version of the American Joint Committee on Cancer staging system for cutaneous melanoma (1).

Once the sentinel lymph node is removed, accurate nodal staging depends on the ability to detect metastatic disease in the lymphatic tissue. To this end, mainly two approaches have been used thus far, histopathologic examination of tissue sections and reverse transcriptase-PCR detection of melanoma specific mRNA sequences. The detection rate for melanoma cells in tissue sections of sentinel lymph nodes by histopathology ranges between 9% and 34% depending on patient characteristics, the number of tissue sections examined, and whether or not immunohistochemistry is applied (2–5). Therefore, whereas histopathologic screening of 139 serial tissue sections enables the detection of ~ 10 tumor cells in a lymph node (6, 7), it would be too laborious to be done routinely. It is evident that the drawback of histopathology limited to a few sections depends on the unpredictable spatial distribution of the tumor within the sentinel node. In theory, PCR-based methods should overcome this problem by completely homogenizing the sample. They rely on mRNA isolation from lysed lymph node tissue and on targeting of melanoma associated mRNA sequences such as tyrosinase, Melan A (Mart 1), and gp100 (HMB45). However, although reverse transcriptase-PCR methods result in higher detection rates than histopathology (up to 70%; refs. 8, 9), they are prone to false positives due to marker gene expression by melanophages, intranodal nerves, benign naevus cells, and illegitimate gene expression of marker genes by other nonmelanocytic cells.

**Authors' Affiliations:** <sup>1</sup>Universitäts-Hautklinik, Eberhard-Karls-Universität, Tübingen, Germany <sup>2</sup>Institut für Immunologie, Ludwig-Maximilians-Universität, Munich, Germany <sup>3</sup>Institut für Pathologie, Eberhard-Karls-Universität, Tübingen, Germany and <sup>4</sup>Institut für Medizinische Biometrie, Eberhard-Karls-Universität, Tübingen, Germany

Received 9/29/04; revised 3/2/05; accepted 3/9/05.

**Grant support:** University of Tübingen grants 787-0-0 and 78-0-0, the Wilhelm Sander Stiftung grant 2003.005.1, and the BioFuture grant 0311884 from the Bundesministerium für Bildung und Forschung.

The costs of publication of this article were defrayed in part by the payment of page charges. This article must therefore be hereby marked *advertisement* in accordance with 18 U.S.C. Section 1734 solely to indicate this fact.

**Note:** J. Fischer is presently at the Universitäts-Hautklinik, Eberhard-Karls-Universität, 72076 Tübingen, Germany.

**Requests for reprints:** Christoph Klein, Institut für Immunologie, Goethestr. 31, 80336 München, Germany. Phone: 89-5996-696; Fax: 011-49-89-5996-696; E-mail: christopher.klein@med.uni-muenchen.de.

© 2005 American Association for Cancer Research.

**Table 1.** Patient characteristics

Patient characteristics	No. patients (%)
Total analyzed	358 (100)
Gender	
Female	157 (44)
Male	201 (56)
Age	
Median, 57	
Range, 11-88	
Site of primary melanoma	
Extremities	169 (47)
Trunk	164 (46)
Head and neck	25 (7)
Histologic type	
Superficial spreading melanoma	187 (52)
Nodular melanoma	85 (24)
Lentigo malignant melanoma	9 (3)
Acral lentiginous melanoma	45 (13)
Not specified	32 (9)
Breslow's tumor thickness	
Median, 1.8 mm	
Range, 0.35-20 mm	
T1	29 (8)
T2	167 (47)
T3	114 (32)
T4	39 (11)
Not specified	9 (3)
Ulceration	
Yes	92 (26)
No	252 (70)
Not specified	14 (4)

Here we present a novel strategy for melanoma cell detection that uses immunocytochemical, microscopic identification of melanoma cells in disaggregated sentinel lymph nodes, thus avoiding false positives resulting from illegitimate mRNA transcription and sampling errors resulting from examination of a limited number of slides. We verify the neoplastic origin by isolation of single positive cells and their genomic analysis using comparative genomic hybridization (10, 11). Thereby, we show that in a substantial number of clinically early-stage melanoma patients genomically aberrant tumor cells can be detected in sentinel lymph nodes that were classified to be free of tumor cells by routine histopathology.

**Patients and Methods**

**Patients.** We included 494 sentinel lymph nodes from 358 patients with clinical early-stage cutaneous malignant melanoma who underwent lymphatic mapping and sentinel lymph node biopsy at the University of Tuebingen from February 2000 until July 2003. Patient data and characteristics of the primary tumor are summarized in Table 1. Staging was done according to the American Joint Committee on Cancer guidelines from 2001 (1). The Tuebingen Ethics Committee approved all aspects of the presented study.

**Lymphatic mapping and sentinel lymph node biopsy.** Preoperatively, a cutaneous lymphoscintigraphy was done after intracutaneous injection of 100 MBq (3 mCi) <sup>99m</sup>Tc-labeled nanocolloids. The technique was supplemented by injection of 1 to 2 mL isosulfan blue dye (Patent blue-V, Altana Pharma, Konstanz, Germany). Sentinel lymph nodes were detected by significant *in vivo* radioactivity and/or by the presence of blue dye in the afferent lymphatic vessels of the sentinel lymph node or the sentinel lymph node itself. For accurate localization of radiolabeled lymph nodes, a hand-held  $\gamma$  probe (C-Trak, Care, Wise Medical Products, Morgan Hill, CA) was used intraoperatively.

**Preparation of the lymphatic tissue and histopathologic examinations.** The lymph node was cut along its longitudinal axis. One half of the sentinel lymph node was fixed in 3.5% formaldehyde, paraffin-embedded, and subjected to standard histopathologic work-up which included H&E staining and immunohistochemistry on three paraffin sections from one central level. For immunostaining, antibodies against HMB-45 or Melan A and S-100 (DAKO, Hamburg, Germany) were used and detected according to the avidin-biotin-peroxidase technique.

**Lymph node disaggregation and immunocytochemistry of disaggregated sentinel lymph nodes.** For immunocytochemistry, the unfixed lymphatic tissue was cut into 1-mm pieces and disaggregated mechanically into a single-cell suspension by rotating knives (DAKO Medimachine, DAKO), washed with HBSS (Life Technologies, Heidelberg, Germany) and centrifuged on a density gradient made of a 60% Percoll solution (Amersham, Uppsala, Sweden). Cells were counted using a Neubauer counting chamber. Per slide, 10<sup>6</sup> cells from the interphase were then given onto adhesion slides (Menzel, Braunschweig, Germany) in a volume of 1 mL PBS. After sedimentation for 1 hour, the slides were air-dried overnight. Immunocytologic staining was carried out with the alkaline phosphatase-anti-alkaline phosphatase method using primary antibodies against gp100 (HMB45, DAKO) and Melan A (A103, DAKO) as primary antibodies and 5-bromo-4-chloro-3-indolyl phosphate/NBT (DAKO) as substrate, yielding a blue reaction product. A lymph node was defined as HMB45 positive and Melan A positive if it contained at least one HMB45-positive and one Melan A-positive cell, respectively. The number of positive cells per million lymphocytes was recorded without knowledge of the histopathologic findings. Positive preparations were air-dried or stored for a maximum of 4 days in PBS until cell isolation for genomic analyses.

**Controls.** Sixty-seven lymph nodes from 59 patients without malignant melanoma were examined immunocytologically after mechanical disaggregation of the lymphatic tissue. Forty-four lymph



**Fig. 1.** Detection of HMB45- and Melan-positive cells in sentinel lymph nodes. **A**, HMB45-positive cell in a histopathologically negative sentinel lymph node. **B**, Melan A – positive cell in a sentinel node of a melanoma patient. **C**, Melan A – positive cell in a lymph node of a control patient (all stained by alkaline phosphatase/anti-alkaline phosphatase, 5-bromo-4-chloro-3-indolyl phosphate/NBT  $\times$  160).

nodes had been removed during crosssection in patients who underwent long saphenous vein stripping for chronic venous insufficiency, 17 lymph nodes due to bronchial carcinoma, and six lymph nodes were excised from patients with nonmelanoma skin cancer. All lymph nodes had at least one million cells available for evaluation and were stained with the antibody HMB45. Fifty-five of these lymph nodes contained at least two million cells and were additionally stained with the antibody Melan A.

**Single-cell comparative genomic hybridization.** For confirmation of the neoplastic origin, 30 immunocytologically positive cells from 18 sentinel lymph nodes were isolated by micromanipulation and single-cell comparative genomic hybridization was done as published by Klein et al. (10) with the modifications described by Ulmer et al. (11). In brief, after isolation, proteinase K served to digest cellular proteins, the single-cell genome was digested using the restriction enzyme *MseI*, adaptors were ligated to the 5' overhangs, and the DNA fragments were amplified by PCR resulting in a *MseI* representation of a single-cell genome. These amplicons were labeled and hybridized. Twenty of the cells were isolated from immunocytologically positive but histopathologically negative lymph nodes, 10 cells from immunocytologically and histopathologically positive sentinel lymph nodes. Primary tumors were microdissected and their DNA amplified as the single cells.

**Statistical analysis.** The difference in the proportion of a positive result according to histology and HMB45 immunocytochemistry was assessed by the sign test. The association between the number of HMB45 immunocytologically positive cells (no. HMB45-positive cells) and the probability to detect metastatic disease by histopathology ( $P_{\text{Histo positive}}$ ) was described by a nonlinear regression analysis using a Hill function with a positive lower asymptote:  $P_{\text{Histo positive}} = 0.004 + 0.996 / [1 + (130 / \text{no. HMB45-positive cells})^{0.52}]$ . The variables were estimated by maximum likelihood. The association between the number of HMB45- and Melan A-positive cells per million lymphocytes was described by Pearson's correlation coefficient after adding the constant one and logarithmic transformation. The association between Breslow's tumor thickness of the primary tumor and the probability to detect HMB45-positive cells by immunocytochemistry (HMB45 positive) was calculated by nonlinear regression analysis using the Hill function:  $P_{\text{HMB45 positive}} = 1 / [1 + (2.83 / \text{tumor thickness})^{0.643}]$ . Because this is equivalent to a logistic regression if one takes the logarithms of tumor thickness, it is also possible to calculate the odds ratios for any multiplicative increase of tumor thickness. If more than one sentinel lymph node per patient was suitable for evaluation, the lymph node with the largest number of HMB45-positive cells was selected for use in the statistical analysis. Nine patients were excluded from the evaluation because the thickness of the primary tumor was not available or imprecise. For 154 patients with HMB45-positive lymph nodes, we determined Spearman's correlation coefficient between the thickness of the primary tumor and the number of HMB45-positive cells/million lymphocytes in the sentinel lymph node. To illustrate the positive association, we calculated the principal component line for the logarithms of both variables.

## Results

First, we examined 67 disaggregated control lymph nodes from nonmelanoma patients by immunocytochemistry using the antibody HMB45, 55 of which were additionally stained with an antibody against Melan A. The mean number of cells examined per lymph node was  $1.6 \times 10^6$  for both antibodies. All 67 controls were negative using the HMB45 antibody, whereas three of 55 nodes from nonmelanoma patients were positive for Melan A (5.4%, Fig. 1C).

A total of 494 disaggregated sentinel lymph node samples from 358 patients were examined by HMB45 and Melan A antibodies (Fig. 1) and the results were compared with

**Table 2.** Findings of immunocytochemistry for single cell preparations using antibodies to HMB45 and Melan A and results of histopathologic work-up

Immunocytochemistry		Histopathology		Total (%)
HMB45	Melan A	No. negative patients	No. positive patients	
Positive	Positive	77	40	117 (32.7)
Positive	Negative	40	2	42 (11.7)
Negative	Negative	166	0	166 (46.4)
Negative	Positive	32	1	33 (9.2)
Total (%)		315 (88)	43 (12.0)	358 (100)

histopathology (Table 2). In all cases, histopathology included immunohistology using either HMB45 or Melan A and S-100 antibodies in addition to H&E staining. The mean number of cells examined per disaggregated lymph node was  $1.6 \times 10^6$  for HMB45 and  $1.3 \times 10^6$  for Melan A. HMB45-positive cells were detected in 159 of 358 patients (44%), whereas histopathology was positive in 43 patients (12%). Interestingly, all lymph nodes that were positive by histopathology were also positive by immunocytochemistry using HMB45 or Melan A antibodies. We found a significant correlation between the numbers of HMB45-positive cells and the numbers of Melan A-positive cells per million lymphocytes detected ( $r = 0.85$ ;  $P < 0.0001$ ;  $n = 494$ ; Fig. 2A). Furthermore, we examined the association between the results of HMB45 immunocytochemistry and histopathology (Fig. 2B). One hundred seventeen of 358 patients were solely positive using the HMB45 antibody, whereas only 1 of 358 patients was exclusively detected by histopathology ( $P < 0.0001$  according to the sign test). Using nonlinear regression analysis, we found a statistically significant association between the number of HMB45-positive cells and the result of histopathology. The percentage of positive lymph nodes by histopathology was 16% when HMB45 immunocytochemistry detected between one and 10 cells per million lymphocytes and rose to 75% when  $>1,000$  HMB45-positive cells per million lymphocytes were found.

These results suggested that increasing the number of tissue sections would improve detection rates by histopathology. To test this hypothesis, we selected 13 lymph node samples that had been negative during standard histopathology. Ten additional levels of the paraffin blocks were cut at an interval of 50 to 250  $\mu\text{m}$  (levels 2-11). Three serial sections were cut at each level and stained with the antibodies HMB45, Melan A, and S100. The results reflect both tumor cell heterogeneity for the markers and the limitations of any detection method. All three lymph nodes that had been negative for both antibodies in our immunocytochemical screen after lymph node disaggregation remained negative (data not shown). Of the remaining 300 immunostains, only 36 harbored tumor cells (12%; Fig. 3) and two slides benign nevus cells, resulting in revised histopathologic diagnosis of disseminated melanoma in six nodes and one intracapsular nevus (LN 8). Three lymph nodes (LN 6, 7, 10; Fig. 3) remained histopathologically negative, although we had detected tumor cells in at least one of the two immunocytochemical assays. One lymph node sample (LN 9) that would have escaped our HMB45-based assay

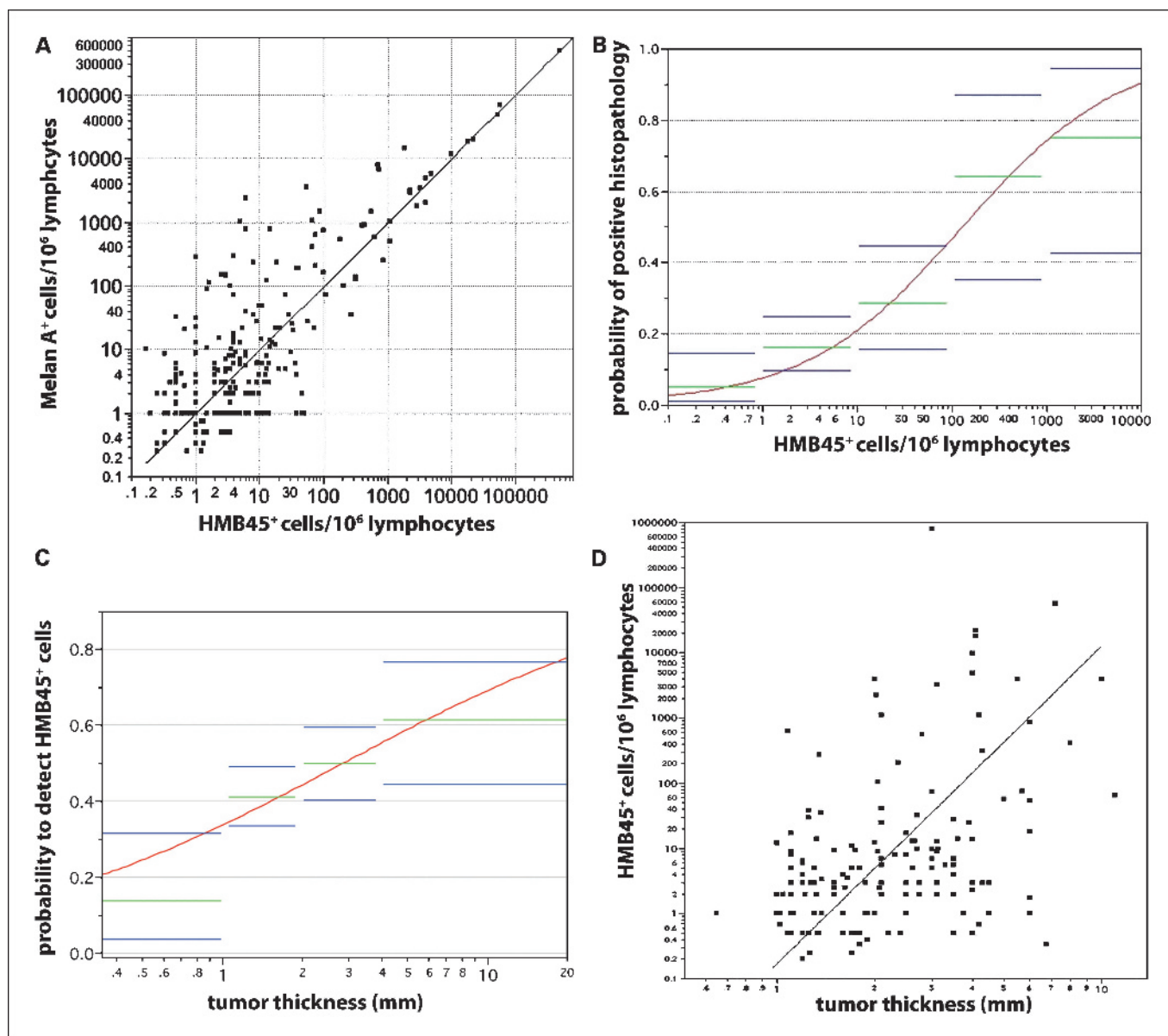


**Fig. 2.** Evaluation of HMB45-positive cells in sentinel lymph nodes. *A*, association between the number of Melan A – and HMB45-positive cells/ $10^6$  lymphocytes ( $r = 0.85$ ;  $P < 0.0001$ ;  $n = 494$ ). *B*, nonlinear regression describing the association between the number of HMB45-positive cells per million lymphocytes detected by immunocytochemistry and the probability to diagnose metastatic disease by routine histopathologic work-up. *Red line*, calculated probability; *green*, actual proportion of histopathologic positivity; *blue*, upper and lower exact 95% confidence interval ( $n = 494$ ). *C*, nonlinear regression analysis showing the association between the thickness of the primary tumor and the probability to detect HMB45 immunocytochemically positive cells in the sentinel lymph node. *Red*, expected; *green*, observed; *blue*, upper and lower 95% confidence interval ( $n = 349$ ). *D*, association between the tumor thickness of the primary tumor and the number of HMB45-positive cells/million lymphocytes detected by immunocytochemistry (HMB45/million;  $r_s = 0.34$ ;  $P < 0.0001$ ;  $n = 154$ ).

however was positive in Melan A immunocytochemistry (Fig. 3). Altogether, we found an excellent association between the extended histopathologic screen and our assay. Using the seven sentinel nodes that were positive by HMB45 immunocytochemistry as reference, we calculated the probability of successful tumor cell detection by histopathology done on four sections from four different levels using the formula  $1 - (1 - q)^4$  for the probability of at least one positive result in four levels if  $q$  is the probability of a positive result for one level. Depending on the antibody selected for histopathologic screening, the probability ranged from 0.22 (HMB45), 0.33 (S100), to 0.37 (Melan A). Therefore, on average, of the seven

HMB45-positive lymph nodes between 1.5 and 2.6 lymph nodes would have been classified positive by histopathology done on sections from four different levels.

Next, we analyzed whether the finding of HMB45-positive cells in the sentinel lymph node correlates with the most important prognostic factor for early-stage melanoma, Breslow's tumor thickness of the primary tumor (Fig. 2C). We found that the number of HMB45-positive nodes increased with greater thickness of the primary tumor ( $P = 0.001$ ,  $n = 349$ ). For a doubling of tumor thickness, the odds ratio for the detection of HMB45 stained cells in a lymph node was 1.56 (95% confidence interval, 1.19-2.04). In addition,

**Fig. 3.** Reexamination of histopathologically negative lymph nodes that were positive in immunocytochemistry. Ten sentinel lymph nodes were analyzed on 10 additional levels for the presence of HMB45-, Melan A-, or S100-positive cells. In total, 300 tissue sections were screened. LN, lymph node; LN dis + IC, number of positive cells detected after lymph node disaggregation and immunocytochemistry; L2-L11, level from which sections were taken; black box, tumor cells in section; white box, no tumor cells present; grey box, intracapsular nevus cells.

	LN	LN dis + IC	L 2	L 3	L 4	L 5	L 6	L 7	L 8	L 9	L 10	L 11
<b>HMB45</b>	1	322										
	2	229										
	3	101										
	4	10										
	5	4										
	6	32										
	7	1										
	8	0										
	9	0										
	10	0										
<b>Melan A</b>	1	139										
	2	317										
	3	162										
	4	1										
	5	2										
	6	24										
	7	0										
	8	3										
	9	8										
	10	3										
<b>S100</b>	1	n.d.										
	2	n.d.										
	3	n.d.										
	4	n.d.										
	5	n.d.										
	6	n.d.										
	7	n.d.										
	8	n.d.										
	9	n.d.										
	10	n.d.										

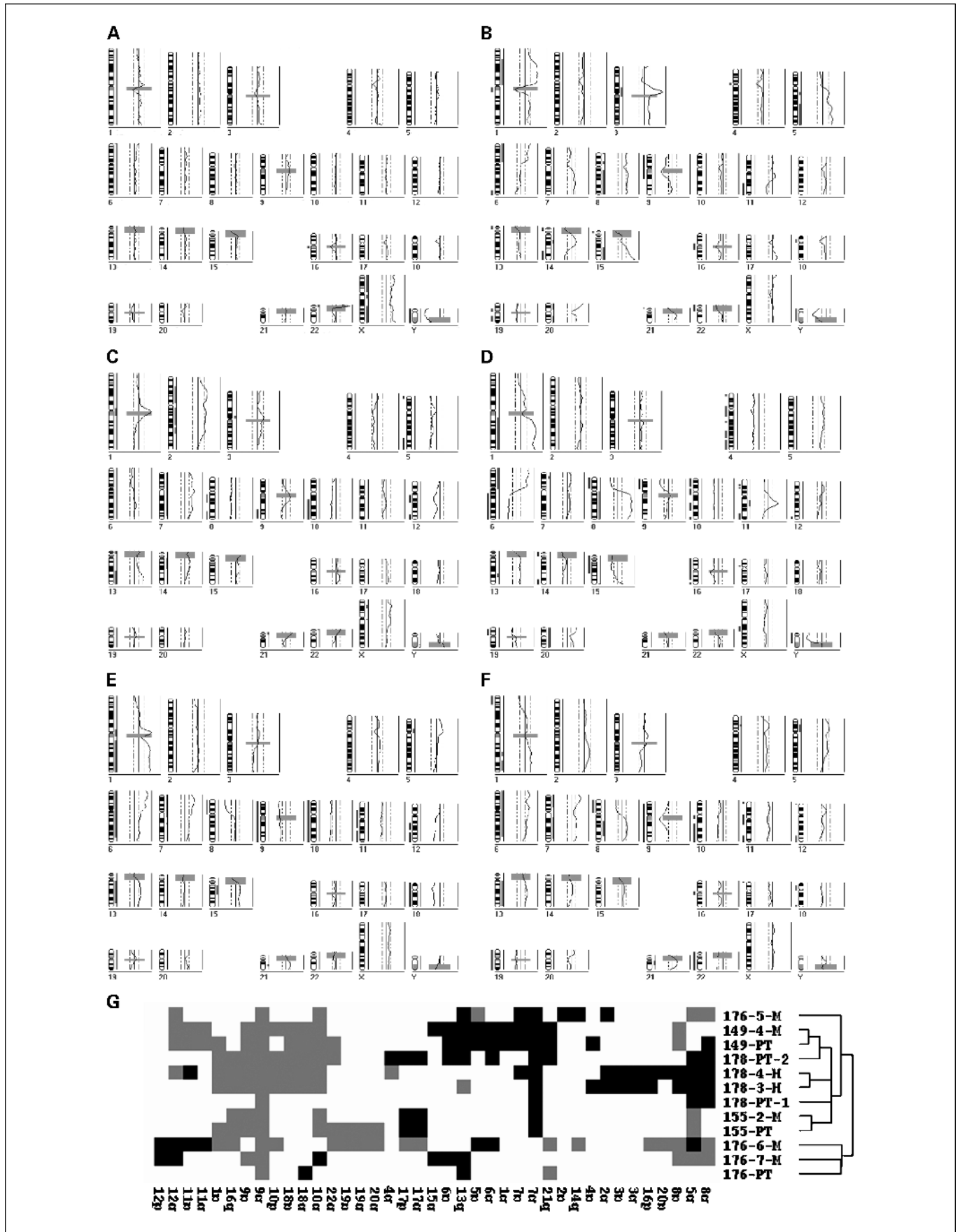
for the HMB45 immunocytologically positive nodes, we could show a significant correlation between the tumor thickness of the primary tumor and the number of positive cells within the sentinel lymph node ( $r = 0.34$ ;  $P < 0.0001$ ,  $n = 154$ ; Fig. 2D).

To confirm the neoplastic origin of the immunocytologically positive cells, we did single-cell comparative genomic hybridization with 30 HMB45- or Melan A-positive cells derived from 18 sentinel lymph nodes and, as control, with seven unstained cells. All unstained cells displayed balanced profiles (Fig. 4A) showing that artificial chromosomal imbalances are rarely introduced by the amplification and hybridization technique. We detected chromosomal aberrations in 24 of 30 (80%) isolated cells (Fig. 4B-E). The most frequent chromosomal aberrations are listed in Table 3. Interestingly, 15 of 24 chromosomally abnormal cells had been isolated from histopathologically negative nodes. Six of the isolated cells that were analyzed by comparative genomic hybridization showed balanced comparative genomic hybridization profiles, suggesting either that sometimes nonmalignant cells will be detected by the assay or that melanoma cells may disseminate before chromosomal aberrations are acquired. Finally, in an

attempt of a first genomic evaluation, we applied hierarchical cluster analysis to four matched pairs of primary tumors and disseminated melanoma cells (Fig. 4E-G). Disseminated tumor cells and their primary tumors were grouped closely together (Fig. 4G), suggesting clonal relationship and confirming the malignant descent of the isolated cells.

### Discussion

The status of the sentinel lymph node is the most important prognostic factor for patients with clinical early-stage melanoma (1). However, the examination of the sentinel lymph node by histopathology is –for practical reasons- usually limited to few tissue sections. Currently, the Association of Directors of Anatomic and Surgical Pathology carefully recommends screening of “more than one section” without specifying concrete numbers (12). A consensus on this issue would be important because it is known that tumor cell detection by histopathology, even when aided by immunohistology, is prone to stochastic errors (6, 7). Sampling errors are frequent because tumor cell detection requires to a large degree the presence of cell clusters, which are however not homogeneously distributed within a



Downloaded from <http://aacrjournals.org/clinccancerres/article-pdf/11/15/5425/1957829/5425-5432.pdf> by guest on 14 December 2024

**Table 3.** The most frequent chromosomal aberrations detected by comparative genomic hybridization in 24 immunocytochemically positive single cells

Chromosomal region	Frequency* (%)
+1q	5 (21)
+6p	11 (46)
+7q	6 (25)
+8q	9 (38)
+13q	7 (29)
+15q	9 (38)
+20p	6 (25)
+ 20q	8 (33)
-6q	8 (33)
-8p	5 (21)
-9p	14 (58)
-9q	10 (42)
-10p	6 (25)
-10q	9 (38)
-11q	6 (25)
-13q	5 (21)

\*Only aberrations that occurred in >20% of samples are listed.

lymph node. This prompted us to test an alternative approach. To overcome the clustered spatial distribution of tumor cells within a lymph node, we prepared single-cell suspensions and screened a large portion of the submitted tissue by immunocytochemistry. This approach averages the number of tumor cells within the cell population.

In a study population of 494 sentinel lymph nodes from 358 patients with early-stage melanoma, we compared the detection rate for melanoma cells between histopathology and immunocytochemistry after disaggregation of the lymph node tissue. For immunocytochemistry on disaggregated lymph nodes, we used two different antibodies, HMB45 and Melan A. Whereas results obtained from the HMB45 and Melan A immunocytochemical assays correlated significantly, their detection rates were significantly higher than that obtained by histopathology. Because HMB45 immunocytochemistry, in contrast to Melan A, never detected positive cells in control lymph nodes, we favor the use of this antibody for tumor cell detection after lymph node disaggregation. Most likely, Melan A-positive cells in control nodes represent nevocellular aggregates that have been previously described using histopathologic examination techniques (2, 5, 13).

The following findings support the conclusion that HMB45 immunocytochemistry indeed detects tumor cells and is superior to standard histopathology. First, we found significant correlations between HMB45 cell numbers and a positive

histopathologic result. Second, most sentinel nodes that were classified as negative by standard histopathologic screening became positive when we analyzed 30 additional sections per node. However, a tolerable routine procedure applied to four sections from four different levels would detect only between 22% and 37% of lymph nodes that are positive by HMB45 immunocytochemistry on disaggregated lymph nodes. Then, we revealed a significant correlation between our assay and Breslow's index of tumor thickness, and finally we confirmed the malignant origin by direct genomic analysis of single isolated cells.

The detection rate of melanoma cells reported here is higher than previously published studies based on standard routine histopathology and is within the range of extensive serial sectioning (14). For the moment, the most relevant question, whether or not increased sensitivity will translate into more precise prognosis of patient outcome, cannot be answered. Because median follow-up time of our cohort currently is only 30 months, we have to wait at least two more years according to estimates that were deduced from previous studies (15). However, we expect a prognostic effect of our assay because of two reasons. First, in contrast to PCR-based studies, our assay enables quantifying tumor cell numbers and therefore the definition of a critical threshold. Such a threshold was recently observed for melanoma cells circulating in the peripheral blood of metastatic patients (11). Second, our approach enables to isolate and characterize even single tumor cells for chromosomal or other genetic aberrations. Whereas a whole genome screen of single disseminated melanoma cells is very labor intensive, data obtained from sufficient numbers of patients might define specific changes or patterns that confer prognostic information. For example, when we screened the whole genome of individually isolated HMB45 or Melan A-positive cells, we discovered various genetic changes and different degrees of chromosomal instability, although the pattern of chromosomal imbalances was highly consistent with cytogenetic and comparative genomic hybridization data from primary malignant melanomas (16, 17). Direct comparison of disseminated cells and their matched primary tumors revealed substantial similarity. However, whereas 80% of the cells showed chromosomal aberrations within the detection limit of comparative genomic hybridization (10-20 Mb), 20% of HMB45- or Melan A-positive cells displayed normal karyotypes. Because five of six of these cells were detected by the HMB45 antibody that never stained cells in control samples, it is not unlikely that they represent tumor cells that disseminated before the acquisition of chromosomal abnormalities detectable by comparative genomic hybridization. Disseminated tumor cells that display normal karyotypes have also been observed for breast cancer and were subsequently identified as tumor cells by methods with higher resolution (18). In addition, 4% of primary melanomas, some of which metastasized later on (19), were found to display

←

**Fig. 4.** Comparative genomic hybridization of isolated single cells and of a matched primary tumor. *A*, unstained control cell. HMB45-positive (*B*) and Melan A-positive cell (*C*) from histopathologically negative lymph nodes. HMB45-positive (*D*) and Melan A-positive (*E*) cell from histopathologically positive lymph nodes. *F*, matched primary tumor for the cell shown in (*E*). To be considered significant, deviations from the central line have to cross the dotted lines indicating the threshold of significance. Regions of chromosomal losses and gains are indicated by bars next to the ideogram of each chromosome (losses, left; gains, right). Gray shaded horizontal bars, regions excluded from analysis because of the prevalence of heterochromatic DNA. *G*, hierarchical cluster analysis of four primary tumors and their matched disseminated cancer cells. The cells are grouped according to similarity of chromosomal aberrations by hierarchical clustering (average linkage mode). Sample identifiers consist of patient numbers, PT for primary tumors, H for HMB45-positive cells, M for Melan A-positive cells. Black box, loss; grey box, gain; white, no aberration.

normal karyotypes. Therefore, it has to be investigated whether disseminated melanoma cells with and without chromosomal abnormalities have different metastatic potential and different prognostic effect. On the other hand and of immediate clinical implication, it should be noted that some melanoma cells isolated from lymph nodes that contained only one or two HMB45-positive cells harbored the almost complete set of genomic aberrations characteristic for fully metastatic cells. Patients with such cells might be at particular risk for metastatic relapse despite negative histopathologic report of their sentinel lymph node.

In summary, the approach presented here enables time and cost-effective, simple and highly sensitive detection of disseminated melanoma cells in sentinel lymph nodes and has the potential to support the identification of those genomic changes and molecular mechanisms that underlie progression to lethal systemic disease.

### Acknowledgments

We thank Ursel Schiebel for excellent technical assistance.

### References

1. Balch CM, Buzaid AC, Soong SJ, et al. Final version of the American Joint Committee on Cancer staging system for cutaneous melanoma. *J Clin Oncol* 2001; 19:3635–48.
2. Abrahamsen HN, Hamilton-Dutoit SJ, Larsen J, Steiniche T. Sentinel lymph nodes in malignant melanoma: extended histopathologic evaluation improves diagnostic precision. *Cancer* 2004;100:1683–91.
3. Cook MG, Green MA, Anderson B, et al. The development of optimal pathological assessment of sentinel lymph nodes for melanoma. *J Pathol* 2003; 200:314–9.
4. Gogel BM, Kuhn JA, Ferry KM, et al. Sentinel lymph node biopsy for melanoma. *Am J Surg* 1998;176: 544–7.
5. Yu LL, Flotte TJ, Tanabe KK, et al. Detection of microscopic melanoma metastases in sentinel lymph nodes. *Cancer* 1999;86:617–27.
6. Gietema HA, Vuylsteke RJ, de Jonge IA, et al. Sentinel lymph node investigation in melanoma: detailed analysis of the yield from step sectioning and immunohistochemistry. *J Clin Pathol* 2004;57: 618–20.
7. van Diest PJ. Histopathological workup of sentinel lymph nodes: how much is enough? *J Clin Pathol* 1999;52:871–3.
8. Bieligg SC, Ghossein R, Bhattacharya S, Coit DG. Detection of tyrosinase mRNA by reverse transcription-polymerase chain reaction in melanoma sentinel nodes. *Ann Surg Oncol* 1999;6:232–40.
9. Wang X, Heller R, VanVoorhis N, et al. Detection of submicroscopic lymph node metastases with polymerase chain reaction in patients with malignant melanoma. *Ann Surg* 1994;220:768–74.
10. Klein CA, Schmidt-Kittler O, Schardt JA, Pantel K, Speicher MR, Riethmuller G. Comparative genomic hybridization, loss of heterozygosity, and DNA sequence analysis of single cells. *Proc Natl Acad Sci U S A* 1999;96:4494–9.
11. Ulmer A, Schmidt-Kittler O, Fischer J, et al. Immunomagnetic enrichment, genomic characterization, and prognostic impact of circulating melanoma cells. *Clin Cancer Res* 2004;10:531–7.
12. Lawrence WD. ADASP recommendations for processing and reporting of lymph node specimens submitted for evaluation of metastatic disease. *Virchows Arch* 2001;439:601–3.
13. Baisden BL, Askin FB, Lange JR, Westra WH. HMB-45 immunohistochemical staining of sentinel lymph nodes: a specific method for enhancing detection of micrometastases in patients with melanoma. *Am J Surg Pathol* 2000;24:1140–6.
14. Scolyer RA, Thompson JF, McCarthy SW. Sentinel lymph nodes in malignant melanoma: extended histopathologic evaluation improves diagnostic precision. *Cancer* 2004;101:2141–2; author reply 2142–3.
15. Kammula US, Ghossein R, Bhattacharya S, Coit DG. Serial follow-up and the prognostic significance of reverse transcriptase-polymerase chain reaction – staged sentinel lymph nodes from melanoma patients. *J Clin Oncol* 2004;22:3989–96.
16. Bastian BC, LeBoit PE, Hamm H, Brocker EB, Pinkel D. Chromosomal gains and losses in primary cutaneous melanomas detected by comparative genomic hybridization. *Cancer Res* 1998;58:2170–5.
17. Mertens F, Johansson B, Hoglund M, Mitelman F. Chromosomal imbalance maps of malignant solid tumors: a cytogenetic survey of 3185 neoplasms. *Cancer Res* 1997;57:2765–80.
18. Schmidt-Kittler O, Ragg T, Daskalakis A, et al. From latent disseminated cells to overt metastasis: genetic analysis of systemic breast cancer progression. *Proc Natl Acad Sci U S A* 2003;100:7737–42.
19. Bastian BC, Olshen AB, LeBoit PE, Pinkel D. Classifying melanocytic tumors based on DNA copy number changes. *Am J Pathol* 2003;163: 1765–70.